1967

Static behavior of composite beams with variable load position, March 1967

J. H. Daniels

J. W. Fisher

STATIC BEHAVIOR OF COMPOSITE BEAMS WITH VARIABLE LOAD POSITION

by

J. Hartley Daniels

and

John W. Fisher

This work has been carried out as part of an investigation sponsored jointly by the New York Department of Public Works, the Department of Commerce - Bureau of Public Roads, Nelson Stud Division of Gregory Industries, Inc., KSM Products Division of Omark Industries Inc., Tru-Weld Division of Tru-Fit Screw Products Inc., and Lehigh University.

March 1967

Fritz Engineering Laboratory
Department of Civil Engineering
Lehigh University
Bethlehem, Pennsylvania.

Fritz Engineering Laboratory Report No. 324.3

TABLE OF CONTENTS

ABSTRACT

The purpose of the two ultimate strength tests which are described in this report was two-fold:

(1) To determine whether a simple span composite beam, subjected to a single concentrated load, could resist the load which would develop the ultimate flexural strength as it passed across the beam from the support to the position of maximum moment, and

(2) To establish the ultimate flexural strength of the cross-section. This was used in the analysis of other test results which are reported in Ref. 4.

Based on the tests described in this report, it was concluded that the ultimate load can pass across a composite beam without a shear failure occurring in the shear connection.

1.0 INTRODUCTION

The proposed procedure [1,2] for the static design of shear connectors for composite steel-concrete bridge beams is based on two criteria:

(1) The flexural strength of a composite beam can be developed if a sufficient number of shear connectors is provided to resist the maximum horizontal force in the slab (maximum slab force), and

(2) The spacing of the shear connectors is not critical; shear connectors can be spaced uniformly without a deleterious effect on the ultimate strength.

The maximum horizontal force in the slab of a simple span composite beam will be determined by the stress distribution on the cross-section at the ultimate moment. If the composite beam is uniform, the slab force will vary from zero at the supports to a maximum value near the applied loads. For such a beam under a single concentrated load at the mid-span, the proposed design procedure would require a sufficient number of uniformly spaced shear connectors in each half of the span to develop the maximum slab force.

A similar analysis would also apply to a simple span composite beam under more than one concentrated load. A composite bridge beam subjected to truck wheel loads would be an example of that load condition. However, for bridge beams, it is of primary concern that the maximum load be able to move into the position which would produce the maximum moment without a failure of the shear connectors.

The purpose of this investigation was to provide experimental evidence of the ability of a simple span composite beam under a single concentrated load, to resist the ultimate load as it passed across the beam from the support to the mid-span. Two beams with identical cross-sections were tested. In the first beam test, the load producing the ultimate moment was placed at the mid-span. In the second beam test, the same ultimate load was placed at five successive positions between the support and the mid-span. The shear connectors in each beam were identical and were designed in accordance with the flexural requirements proposed in Refs. 1 and 2.

These tests were conducted during the same period of time as the static tests of four continuous composite beams which were reported in Refs. 3 and 4. To assist with the analysis of those test results, the span lengths of the simple and continuous beams were made the same and a constant cross-section was used in the positive moment regions of all of the beams.

2.0 TEST BEAMS, INSTRUMENTATION AND TESTING PROCEDURE

2.1 Description of Beams

The two composite beams tested in this investigation were designated SC-1S and SC-2S. They were each 25' - 10" long overall with a single span of 25' - 0" between bearings. The beams consisted of a reinforced concrete slab 60-in. wide and 6-in. thick connected to a 21W62 steel beam by pairs of 3/4-in. stud shear connectors 4-in. high. Details of the composite beams are shown in Figs. 1 and 2.

2.2 Design Criteria

The cross-sections of beams SC-1S and SC-2S were made the same as the cross-sections at the load points of the four continuous composite beams reported in Refs. 3 and 4. The maximum load capacity was computed using ultimate strength theory.

The shear connectors for beams SC-1S and SC-2S were proportioned in accordance with the flexural strength criterion proposed in Ref. 2 using the reduction factor proposed in Ref. 1. The shear connector spacing for both beams is shown in Fig. 3.

2.3 Design Details and Fabrication

The details of the steel beams are shown in Fig. 3. The two beams were cut from a single 57-ft. rolled section by a local fabricating shop. This steel beam and the four steel beams reported in Refs. 3 and

4 were supplied from the same heat of A36 steel. The excess pieces after cutting, were marked and delivered to Fritz Laboratory after all shear connectors were installed, to provide material for tension tests of the steel section and of the studs. Bearing stiffeners were fitted and welded to the beams by the fabricating shop.

All 3/4-in. studs were installed in pairs. Before studs were welded to the test beams the stud welding equipment was calibrated by welding several studs to the excess lengths of beam that were cut off. The quality of the welds was verified using the welding and inspection procedure outlined in Ref. 5. Two different lots of 3/4-in. by 4-in. studs were installed. They were supplied by two manufacturers. Beam SC-1S had lot A studs and beam SC-2S had lot B studs (Ref. 3, page 12). This choice was randomly made.

2.4 Construction

Composite beams SC-1S and SC-2S were constructed at the same time as continuous beams CC-1F and CC-2F (Refs. 3 and 4). The four steel beams were placed in two parallel lines 75-ft. long and 5" - 2" apart. They were clamped to steel supports which were bolted to the dynamic test bed.

Plywood forms for the slabs of the four T-beams were suspended from the steel beams. A two-inch timber bulkhead was used to separate the slabs of the two lines of T-beams along their length and to separate the continuous and simple span beams. Figure 4 shows the formwork and reinforcement for the slabs of beams SC-1S and SC-2S and the start of concrete pouring. In the lower photo of Fig. 4, the formwork and reinforcing for beams CC-1F and CC-2F begins at the bulkhead just behind the hopper discharging the concrete for beams SC-1S and SC-2S. The slabs of the four beams were poured in a continuous operation beginning with beams SC-1S and SC-2S.

The concrete for the slabs was transit - mixed and proportioned for a 28-day compressive strength of 3000 psi. Consolidation was accomplished by internal vibration along the slab as placement progressed. The final finsih was made by hand trowelling. Eleven test cylinders were poured during the casting of beams SC-1S and SC-2S.

The concrete in the slabs of beams SC-1S and SC-2S was moist-cured for seven days. The exposed surface was covered with wet burlap and a polyethylene sheet. The forms for the two beams were removed approximately 14 days after casting and the specimens were allowed to cure under dry conditions until tested.

2.5 Properties of the Test Beams

A test program was conducted to determine the mechanical properties of the materials used in the T-beams. The physical dimensions were also obtained to help ascertain the section properties of the composite beams.

The rolled steel beams were made of structural carbon steel meeting the requirements of ASTM A36 - 63T. The mill report is given in Table 1.

The mechanical properties of the structural steel were determined from test coupons cut from a 2-ft. long piece of beam that had been left over when the 57-ft. long rolled section had been cut to length. The coupons were tested in tension at a speed of 0.050-in. per minute to fracture. In all tests, the yield point, static yield level and ultimate load were measured, and their mean values are shown in Table 2. The modulus of elasticity was determined from a stress-strain curve which was plotted automatically during the test. The strain hardening modulus was not obtained.

Although all five rolled beams were supplied from the same heat of A36 steel, as previously mentioned, the values shown in Table 2 are noticeably lower than the values given in Table 3 of Ref. 3 for the other four beams.

The mechanical properties of the No. 4 deformed longitudinal reinforcing bars were determined by tension tests of 3-ft. lengths of reinforcement. The tests were representative of all No. 4 bars used in the slabs of the simple span beams reported herein and the continuous beams reported in Refs. 3 and 4. The values shown in Table 2 were obtained from Table 3 of Ref. 3.

The mechanical properties of the stud shear connectors are also shown in Table 3 of Ref. 3.

The concrete used for the slabs of beams SC-1S and SC-2S was made of Type 1 portland cement, crushed gravel and natural bank sand. These slabs were poured at the same time as the slabs for beams CC-1F and CC-2F (Ref. 3). Eleven standard 6" X 12" cylinders were made during the casting of slabs for beams SC-1S and SC-2S. These cylinders were tested at the age of 28 days and at the beginning of each ultimate strength test.

The compressive strengths, splitting strengths and moduli of elasticity are given in Table 3.

The cross section properties of the 21W62 rolled steel beams used in beams SC-1S and SC-2S are shown in Table 4. The properties are based on measured dimensions and are compared with standard handbook values.

Cross-section properties of the composite sections were computed on the basis of the cross-section dimensions and the material properties. Table 5 gives the moments of inertia, distance to the neutral axis from the bottom of the beam, and the ultimate moment capacity of each beam.

2.6 Instrumentation

The instrumentation of beams SC-1S and SC-2S was essentially the same as the instrumentation of beams CC-1F and CC-2F. Reference 3 provides the details for the latter two beams. Figures 5 and 6 summarize the details of the instrumentation used for the test beams in this investigation. A combination of electrical resistance strain gages, dial gages and level bar rotation gages was used.

Figure 5 shows the location of the electrical resistance strain gages which were used to determine the flexural strains in the steel beams and in the concrete slabs. For beam SC-1S, they were located at two cross-sections, designated 3 and 5. For beam SC-2S, they were located at five cross-sections, designated 1 to 5. The numbered cross-sections also refer to the consecutive load positions on beam SC-2S. The load was placed at mid-span (Section 5) of beam SC-1S.

Figure 6 shows the locations of the dial gages that were used to measure slip and deflection, and the level bars which measured rotation of the beams at the supports. A 0.001-in. dial gage was placed at mid-span (Section 5) of each beam. For beam SC-2S, a 0.001-in. dial gage was also placed consecutively under each of the other load positions (Sections 1 to 4). These dial gages had a range of 2-in. For greater deflections, a 0.01-in. graduated scale was used.

2.7 Test Procedure

Each beam was supported at its ends by 8-in. diameter steel rollers which were bearing on 16-in. high steel supports. The rollers were both free to move as the lower flange extended during loading. Blocks were provided however to prevent sudden movements of the rollers at large deflections. Longitudinal stability was maintained by the cross-head of the testing machine. Load was applied by the 5,000,000 - lb. Baldwin testing machine located in Fritz Laboratory. A 4-ft. long loading beam distributed the load across the slab width to two 22-in. long by 5-in. wide bearing plates which rested against the concrete slab. The ends of the bearing plates cleared the strain gages on the slab surface by 3-in. The test set-up is shown schematically in Fig. 7. During each test, mechanical jacks were installed on either side of the end supports and continually adjusted to a loose bearing against the concrete slab as load was increased. These jacks provided stability of the beam against overturning. The loading and support details can be seen in Figs. 8 and 9.

The test of beam SC-1S was started 32 days after the concrete slab was poured. The beam was moved into position in the testing machine and the load applied at mid-span. The ultimate strength test required approximately 12 hours to complete and was carried out on 2 consecutive days. The load was increased in relatively small increments in the elastic range, then held constant while data was obtained from all instruments. As plastic deformations took place, a longer interval was required before the load increment stabilized and deflections ceased. Generally, 5-min. was required to stabilize the load. All data corresponding to a given load increment was obtained in approximately 20-min.

In the plastic range, increments of deflection were applied. Generally, 15 to 20-min. were required to allow the test load and deflections to stabilize before data was taken. Since deformation rather than load was used to control the progress of the test, it was possible to obtain data up to and beyond the maximum load capacity of the beam.

The test of beam SC-2S was started 84 days after the concrete slab was poured. The start of this test was delayed by the fatigue and static tests of beams CC-1F and CC-2F (Refs. 3 and 4). The ultimate load determined from the test of beam SC-1S (130 kips) was applied to beam SC-2S at five consecutive positions (Fig. 5) between the West support and midspan. The test procedure was identical to that for beam SC-1S except that the beam was moved after each application of the test load to the next load-position.

The test of beam SC-2S required 5 days to complete. The test load was applied in about 1 to 2 hours at each of the load positions 1 to 4 (Fig. 5). The beam was then moved and the test load applied at the next load position the following day. On the fifth day when the test load at mid-span (position 5), the test required about 8 hours to complete. The load at mid-span was allowed to reach the ultimate strength of beam SC-2S (136 kips) which slightly exceeded the ultimate strength of beam SC-1S.

Figure 9 shows beam SC-2S during and after the test. The test load is shown at positions 1, 4 and 5. The load shown at position 4 had not been completely applied. Therefore, yielding at this section had not yet completely developed. The full extent of yielding in the web in the vicinity of section 3 which resulted from the test load at this section can be seen however. Considerably more yielding occurred at section 4 under the full test load. The extent of slab crushing and the lateral deflection of the tension flange at the ultimate load are clearly visible.

3.0 TEST RESULTS AND ANALYSIS

3.1 Load - Deflection and Ultimate Strength Behavior

Figure 8 shows beam SC-1S following the ultimate strength test. The extent of crushing of the concrete slab at the load point can be clearly seen.

Figure 9 shows beam SC-2S during the ultimate strength test and after application of the ultimate load at mid-span. The load is shown only at positions 1, 4 and 5. The test load shown at position 4 had not been completely applied when the photograph was taken. Therefore, the extent of yielding in the steel beam was greater than is shown. However, the extent of yielding at position 3 is apparent. Considerably more yielding occurred at position 4 than at position 3 when the full test load was applied. The amount of crushing of the concrete slab and the lateral deflection of the tension flange at the ultimate load (load at position 5) are clearly visible.

Deflection measurements were obtained at mid-span of beams SC-1S and SC-2S during the progress of each test. The resulting load-deflection curves are shown in Figs. 10 and 11.

Certain visual observations were made and are noted on each Figure by letters (A) to (E). For beam SC-2S these observations were noted corresponding to the load at mid-span. They were as follows:

(A) Approximate indication of first yielding of the lower flange. A slight amount of yielding occurred in the web at the junction of the lower flange and web below the load prior to this point. In beam SC-2S some yielding of the flange had spread to section 5 when the test load was applied at section 4. When the test load was applied at section 5 of this beam (mid-span), first yielding was taken as the first additional flange yielding at section 5. The theoretical load to cause first yielding at section 5 (assuming zero residual stress) was 80 kips in beam SC-1S and 82 kips in beam SC-2S. This load was based on computed elastic properties of the composite section assuming complete interaction.

(B) The top surface of the concrete slab has begun to crush adjacent to the loading beam.

(C) The concrete slab has crushed to full depth. The extent of crushing can be seen in Figs. 9 and 10.

(D) The tension flange of the wide-flange beam has begun to deflect laterally.

(E) Test terminated due to large lateral deflections of the tension flange and warping of the wide-flange beam at the supports. Figure 12 shows the shape of the cross-section of beam SC-2S at section 5 (mid-span) after the test. Under the load at which the test was terminated, the lateral deflection of the tension flange was about 2-in. greater than that shown in the Figure.

In Fig. 11, the load- deflection curves (mid-span deflection) are shown for each of the load positions 1 to 5. No flange yielding occurred when the test load was applied at sections 1 and 2. Some small yield lines did appear however in the web (Fig. 9) at section 2. Flange and web yielding at sections 3 and 4 occurred when the test load was moved to those positions. A small amount of slab crushing occurred adjacent to the load point when the test load was applied at section 4. This crushing was observed just before the test was terminated.

The ultimate load capacity of beam SC-2S was 136 kips compared with 130 kips for beam SC-1S, a 4.5% increase. The increased load capacity of beam SC-2S can be attributed mostly to two causes; (1) slight differences in material properties and geometry and (2) the increase in concrete strength which occurred during the interval between the two beam tests (Table 3).

A comparison of Figs. 10 and 11 shows significant differences and similarities between the load - deflection curves for the load at mid-span (section 5). These can be summarized as follows:

(1) First yield of the bottom flange (as defined previously) occurred at a load very close to the predicted load for each beam.

(2) The first observed crushing of the top surface of the concrete slab occurred at nearly the same load and deflection in each beam. The load was slightly higher in beam SC-2S.

(3) The deflection of beam SC-2S at which crushing had progressed to the full depth of the slab at section 5, was considerably smaller than in beam SC-1S.

(4) The load and deflection at which the tension flange began to deflect laterally, was nearly the same for both beams.

(5) The final load and delfection at the end of testing was nearly the same for both beams.

It is apparent from this comparison that the gross load - deflection behavior of the two beams was very similar. However, the difference in deflection between first crushing and full depth crushing of the slabs of the two beams at mid-span was significant. The smaller difference which occurred in beam SC-2S most likely can be attributed to overstressing of the concrete near mid-span before the load reached this point. It was observed during the test of SC-2S that when the load was being applied at section 5, some further crushing of the concrete took place at section 4 before first crushing occurred at section 5. Then, crushing at section 5 proceeded rapidly through the slab depth.

It can therefore be concluded on the basis of these two tests that the mid-span load which would develop the ultimate flexural capacity of a uniform simple span composite beam can move from the support to the position of maximum moment. It could also be concluded from the above discussion that the ductility of such a beam under the moving ultimate load would be somewhat less than a similar beam loaded only at midspan. A measure of ductility in this case is the length of the uniform load plateau at the ultimate load.

3.2 Load - Rotation Behavior

Rotation measurements were taken at each end of beams SC-1S and SC-2S during the progress of the tests. The resulting load - rotation curves are shown in Figs. 13 and 14.

Rotations of beam SC-1S (Fig. 13) were recorded only up to a load of 127 kips. This was just short of the ultimate load of 130 kips. The reason was as follows: During the first day of testing a plateau in the load - deflection curve was reached at 127 kips and the test was stopped (Fig. 10). The slip gages and rotation gages were removed when the load first reached 127 kips. The next day it was decided to reload the beam and deform plastically until unloading was evident. The load reached 130 kips and remained constant for a small increase in deflection before unloading began (Fig. 10). No slip or rotation measurement were obtained at this time. The ultimate load of SC-1S was then taken as 130 kips, which was also taken as the test load for beam SC-2S.

Since the mid-span deflection and end rotations are predictably related (under the assumption of elastic-plastic theory) it would be expected that the load - rotation curve of Fig. 13 would behave similar to the load - deflection curve of Fig. 10 in the vicinity of the ultimate load. On this basis, the curve in Fig. 13 was extended (dashed line).

A comparison of Figs. 13 and 14 shows that beam SC-2S has significantly smaller end rotations at the point of unloading. This is in agreement with the load - deflection results discussed previously.

In addition, it can be seen from Fig. 14 that the West end of beam SC-2S is subjected to greater rotations than the East end throughout the test. This result was expected since the West half-span develops inelastic deformations over much of the half-span length as the load moves towards mid-span. Most of the East half-span remains elastic during this time.

3.3 Load - Slip Behavior

Load - slip curves for beams SC-1S and SC-2S are shown in Figs. 15 and 16. Slip was measured between the concrete slab and the steel beam at each end of the two beams. Measurements of slip were not recorded for beam SC-1S beyond a load of 127 kips. The reason for this was mentioned in the discussion of the load - rotation behavior of beam SC-1S.

The slip at each end of beam SC-1S was nearly the same within the region shown in Fig. 15. Much larger slip had developed by the end of testing but was not recorded.

The slips measured at each end of beam SC-2S were significantly different, as expected, until the load was at mid-span and unloading of the beam had begun.

With the test load at positions 1 to 4 of beam SC-2S, the computed value of the horizontal shear to the West of the load-point was greater than it was to the East. Consequently, with equal number of uniformly spaced connectors in each half-span, the computed average force per connector to the West of the load point was greater than it was to the East. Therefore, the West end slips could be expected to be larger than those at the East end, and inelastic deformations could also be expected to start first on the West side of the load as it moves across the span.

Fig. 16 confirms this behavior. Elastic deformation occurred at each end with the load at positions 1 and 2. However, they were much larger at the West end. With the load at position 3, considerable inelastic slip occurred at the West end while the deformation at the East end remained elastic. The first inelastic slip at the East end occurred with the load in position 4.

When the test load of 130 kips was applied at section 5 (mid-span), the East and West slips were considerably different. However, when the load was increased to 136 kips much more inelastic deformation occurred in the East half-span than in the West half-span. As a result, during unloading of beam SC-2S, the East and West end slips were nearly equal.

There was no indication of connector failures during the tests of beams SC-1S and SC-2S, although a visual inspection of the connectors was not made. Table 5 of Ref. 2 lists 21 values of the maximum slip which occurred in stud shear connectors that failed above the weld. The minimum value of slip to produce failure of a 3/4-in. stud connector in a pushout specimen is shown there as 0.246-in. The smallest value shown in the table is 0.092-in. This value occurred with 1/2-in. stud connectors in a beam test. Since the maximum end slip recorded during the tests of beams SC-1S and SC-2S was less than 0.05-in. no stud failures would have been expected.

3.4 Strain Distribution Across the Slabs

Measured strains at the top surface of the concrete slabs of beams SC-1S and SC-2S are shown in Figs. 17 and 18.

Figure 17 shows the strain distribution at positions 3 and 5 of beam SC-1S for the load at mid-span. Strains at position 5 for loads greater than 125 kips could not be obtained. They were considerably larger than at position 3. First crushing of the slab at mid-span of beam SC-1S (position 5) was observed at a load of 127 kips (Fig. 10).

Strains measured at positions 3 and 5 of beam SC-2S are shown in Fig. 18. Two sets of strain distributions are shown; one for the test load at position 3, the other for the test load at position 5. For the test load at position 3, the strains at mid-span were quite small. It is also apparent from Fig. 18 that elastic behavior had occurred in the slab for the load in positions 1 and 2 since there were no residual strains.

Inelastic strains occurred in the slab at positions 3 and 5 when the load was moved to position 4. This can be observed from the residual strains at 3 and 5 at the start of testing when the load was at position 5. Strains at 3 and 5 were obtained up to the ultimate load of 136 kips. First crushing of the slab at mid-span of beam SC-2S was observed at a load of 127 kips (Fig. 11).

Two significant observations can be made from Figs. 17 and 18:

(1) Strains were nearly uniform across the slabs of beams SC-1S and SC-2S at positions 3 and 5 except in the vicinity of the ultimate load at position 5. This indicates that the full slab width was nearly effective up to the ultimate load. The change in distribution at high loads was likely due to transverse bending of the slab at the load point. Previous investigations[6] have discussed the importance of transverse bending of composite beam slabs. The strain distribution is altered in two ways; (1) the curvature parallel to the longitudinal beam axis changes in the transverse direction,

and (2) the change in shape of the cross-section results in a variable distance from the neutral axis to the extreme fibre. The positions of the neutral axis and plastic centroid also vary due to change in shape of the cross-section.

Because of the above effects, the strain distributions at high loads cannot be used as a measure of slab effectiveness if transverse bending occurs.

(2) The strains at the surface of the slab at mid-span of beam SC-2S are somewhat lower than at the same position of beam SC-1S, even though the ultimate load of beam SC-2S was slightly higher. This most likely resulted from the high degree of slip and loss of interaction in the West half-span of beam SC-2S and the crushing of concrete at position 4 which occurred prior to the application of load at mid-span.

3.5 Forces on the Stud Shear Connectors

The horizontal slab force at a position containing the test load was computed from the measured strains on the wide-flange beam at that position. Therefore the slab force was computed at position 5 (mid-span) of beam SC-1S and at each of positions 1 to 5 of beam SC-2S.

Figure 19 shows the computed horizontal slab forces in beams SC-1S and SC-2S. A comparison is made with the cumulative ultimate resistance of the stud shear connectors between any given cross-section and the end of the beam. The upper dashed curve shows the cumulative resistance based on an ultimate strength per 3/4-in. stud connectors of 35.8 kips. This value assumes a concrete strength of 4,000 psi (Ref. 1). The solid curve assumes a value of 28.7 kips per 3/4-in. stud connector which corresponds to 3,000 psi concrete strength. The lower dashed curve is the design cumulative resistance which is obtained by applying the 0.85 reduction factor to the solid curve.

The horizontal slab forces shown at positions 3, 4 and 5 include an estimated increase due to strain hardening. The strain hardening modulus given in Table 3 of Ref. 3 was used for strains exceeding the yield strain of the steel beam. Strain hardening did not occur at positions 1 and 2. The estimated increase in slab force due to strain hardening at positions 4 and 5 was approximately 5% and 15% respectively.

It is apparent from Fig. 19 that the connectors in beam SC-2S were subjected to forces that closely correlated with their design resistance.

3.6 Maximum Flexural Capacity

Figure 20 compares the maximum moment envelopes for the two test beams. Also shown is the ultimate moment capacity envelope along the beam span. This envelope varies from the plastic moment capacity of the steel section at the support to a maximum value equal to the flexural strength of the composite section. The intermediate values of of flexural strength were computed on the basis of an inadequate shear connection as described in Ref. 2 by Slutter and Driscoll. The computations were based on a shear strength of 28.7 kips per stud corresponding to 3,000 psi concrete strength. If a shear strength of 35.8 kips per stud were used (4,000 psi concrete strength) the value of maximum flexural strength would be the same as that shown in Fig. 20 since this level is determined by the static yield stress in the steel beam. However, the distance from the mid-span to the first reduction in capacity would increase and the intermediate values of flexural strength would increase somewhat. The flexural strength at the support would remain unchanged.

As previously mentioned, the computation of the ultimate moment capacity envelope was also based on the static yield strength values of the steel beam given in Table 2. This limits the value of slab force which can develop near the mid-span. Since the static yield stress level was lower than that assumed in the design (36 ksi), the shear force per stud will be less than 28.7 kips in the region near the mid-span. An increase in steel stress due to strain hardening will increase the shear force on the studs near the mid-span resulting in an increased level of ultimate flexural capacity in this region. In fact, if it is assumed that all studs are subjected to their maximum shear capacity of 28.7 kips (up to the limit of the slab capacity itself), the ultimate flexural capacity envelope between sections 3 and 5 will closely approximate the bending moment envelope for beam SC-2S between those sections.

Baldwin (private correspondence with John W. Fisher) suggested that the ultimate moment capacity at any cross-section should always exceed the computed moments at that cross-section. He noted that unlike prismatic beam sections, the ultimate moment capacity varied along the length of the beam because only near the mid-span was the shear connection sufficient to fully develop the section. Based on the earlier discussion it is apparent from Fig. 20 that the flexural capacity was adequate to resist the applied loads at all sections along the beam span. The loads at sections 1, 2 and 3 generated bending moments that were equal to or less than the computed flexural capacity at those sections. The flexural capacity was approximately equal to the applied bending moments at sections 4 and 5.

An examination of Fig. 19 shows that the slab force along the beam had nearly reached the maximum obtainable value at sections 1, 2 and 3. Figure 16 indicates that this force was being maintained during considerable inelastic slip. Additional inelastic slip would be required in order that the applied moments reach the flexural capacity in the region from the support to section 3 (Fig. 20). Slutter and Driscoll[2] have shown that sufficient ductility of the stud connectors was available to allow the flexural capacity to be reached when the ratio of (initial) maximum moment to ultimate moment was as low as 0.8. This corresponded to a ratio of total connector strength (inadequate shear connection) to maximum slab force of about 0.5. These results would indicate that for beam SC-2S sufficient ductility of the stud connectors would exist at least between sections 2 and 3 (Fig. 20) to allow the flexural capacity to be reached. It is doubtful if it would be required to reach the flexural capacity nearer to the support.

As a result it should be possible to depend on the flexural capacity of the sections with inadequate shear connection as suggested by Baldwin.

3.7 Local Buckling

Local buckling of the top flange of the W in beam SC-1S, was observed just prior to the end of the test. At this stage, the concrete had crushed to full depth and the top flange of the steel beam was in compression. The buckle developed only in the half-flange on the south side of the beam. It was located in the West span between the first and second pair of studs from the load point. The buckle was about 10-in. in length and bent away from the slab about one inch. The opposite half-flange on the North side of the beam did not buckle. No local buckling was observed in beam SC-2S.

Local buckling of composite beams is discussed in Ref. 4. In that discussion reference was made to studies in which both half-flanges rotate in the same direction at a local buckle; thus both participate. The local buckle which occurred in beam SC-1S, indicates that in composite beams only one half-flange may buckle, the other being restrained by the concrete slab.

The local buckle in beam SC-1S did not affect the test results since it occurred during unloading of the beam.

4.0 SUMMARY

The results of the static tests of two nearly identical simple span composite steel-concrete beams have been presented in this report. Each beam had a span of 25 feet and consisted of a 60-in. wide by 6-in. reinforced concrete slab connected to a 21W62 A36 steel beam with 3/4 inch diameter by 4-in. high headed steel stud shear connectors. Connectors were designed in accordance with the static requirements of Refs. 1 and 2. One beam was loaded at mid-span to its ultimate load. This load was then applied at five consecutive positions between the support and mid-span of the second beam starting near the support. This loading sequence was intended to simulate a single concentrated moving load equal to the ultimate load of the beam as it travelled from the support to the position of maximum moment (mid-span). When the test load reached the mid-span, it was increased slightly until collapse of the beam occurred.

The following conclusions were drawn from an analysis of the test results:

(1) Simple span composite beams with stud shear connectors designed in accordance with the flexural strength (static) requirements of Refs. 1 and 2, will be able to develop the ultimate flexural strength of the beam as the load passes across the beam from the support to the position of maximum moment.

(2) Although considerable inelastic shear deformations of the studs will occur in the shorter shear span as the load moves across the beam, the slip at the ends of the beam will be below the slip at which stud shear failures could be expected.

(3) The ductility (as defined in the report) of a composite beam subjected to a moving load will be somewhat less than the same beam loaded only at mid-span.

(4) These tests indicate that the flexural capacity of the sections with inadequate shear connection will provide sufficient flexural capacity to allow the ultimate load to pass across the beam.

5.0 ACKNOWLEDGMENTS

The study described in this report was part of an investigation on composite beams that was conducted at Fritz Engineering Laboratory, Department of Civil Engineering, Lehigh University. L. S. Beedle is Acting Chairman of the Department and Director of the Laboratory. The project was financed by the New York Department of Public Works, the Department of Commerce - Bureau of Public Roads, Nelson Stud Division of Gregory Industries, Inc., KSM Products Division of Omark Industries, Inc., Tru-Weld Division of Tru-Fit Screw Products Inc., and Lehigh University.

The writers wish to thank Dr. R. G. Slutter for his advice and help in the planning and conduct of these tests, and to Messrs. K. R. Harpel and C. F. Hittinger and their staff at the Fritz Laboratory for their work in preparing the test set-up and instrumentation; to R. N. Sopko and his staff for preparing drawings and providing the photographic coverage; and to Mrs. D. Eversley for typing the manuscript.

6.0 TABLES AND FIGURES

TABLE 1

MILL TEST REPORT FOR 21W62

Yield Point (KSI)	Tensile Strength (KSI)	Elongation 8-in. %	Chemical Analysis			
			C	M_n	P	S
41.9	67.2	30	0.19	0.70	0.010	0.029

TABLE 2

MATERIAL PROPERTIES OF STEEL

Type of Specimen	No. of Tests	Yield Point (KSI)	Static Yield Stress (KSI)	Tensile Strength (KSI)
		Mean	Mean	Mean
Web* (21W62)	3	34.1	31.6	59.3
Flange* (21W62)	3	34.7	32.5	59.8
No. 4 Bar	2	50.1	47.9	78.4

* Average Modulus of Elasticity, $E = 29.0 \times 10^3$ (KSI)

TABLE 3

RESULTS OF CONCRETE CYLINDER TESTS

Beam	MOIST CURED					DRY CURED			
	No. of Tests	Age (Days)	Splitting Tensile Strength T(psi)	Compressive Strength f'_c (psi)	Modulus of Elasticity E_c ($x10^3$ksi)	No. of Tests	Age (Days)	Compressive Strength, f'_c(psi)	
			Mean	Mean				Mean	Std. Dev.
CC-1S	1	28	610	5,240	3.7	6	32	5,230	250
CC-2S	1	28	610	5,240	3.7	3	84	5,550	-

TABLE 4

BEAM	AREA*	DEPTH	FLANGE WIDTH in.	FLANGE THICKNESS in.	WEB THICKNESS	MOMENT OF INERTIA
SC-1S	18.11	21.08	8.30	0.571	0.433	1281
SC-2S	18.09	21.00	8.31	0.571	0.433	1285
21W62**	18.23	20.99	8.250	0.625	0.400	1327

* BASED ON RECTANGULAR ELEMENTS - FILLETS NEGLECTED

** FROM AISC MANUAL OF STEEL CONSTRUCTION

TABLE 5

PROPERTIES OF COMPOSITE BEAMS

Beam	Moment of Inertia	Position of Neutral Axis from Bottom	Computed Ultimate Moment
	in^4	in	k - in
SC-1S	3650	20.33	8930
SC-2S	3635	20.30	8900

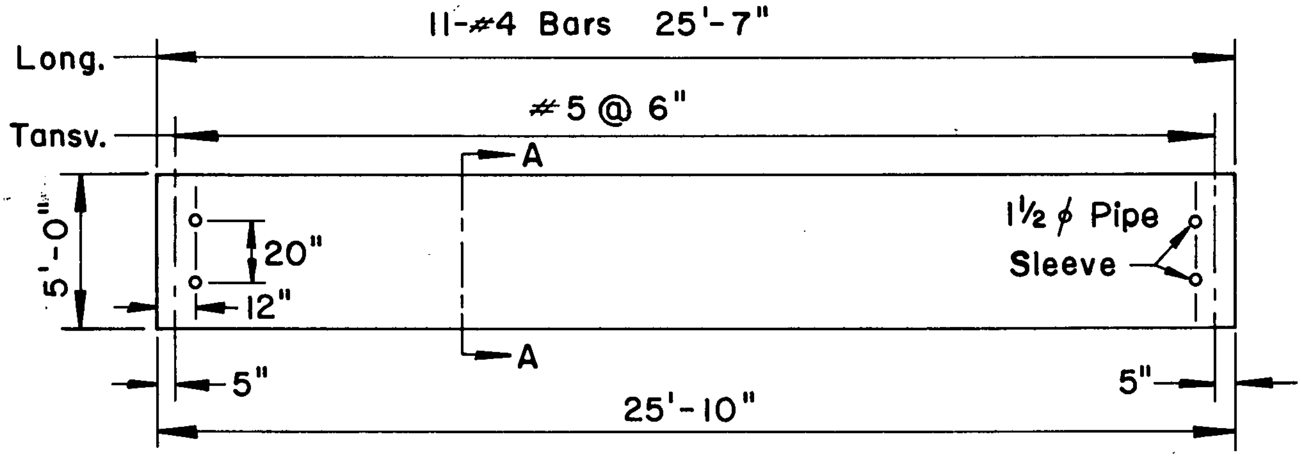

FIG. 1 - DETAILS OF COMPOSITE BEAMS SC-1S AND SC-2S

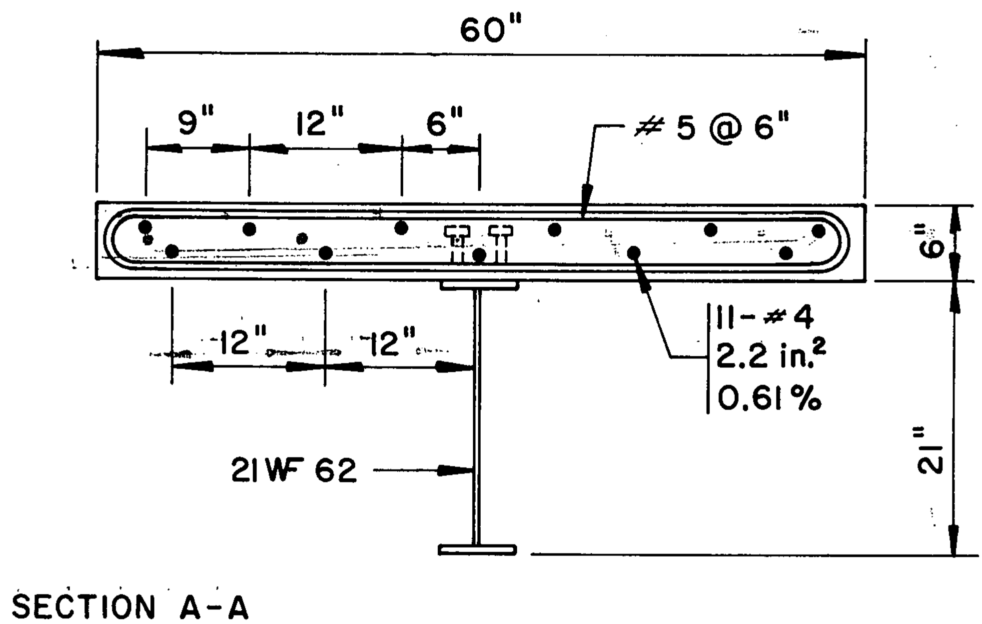

FIG. 2 - TYPICAL BEAM CROSS-SECTION

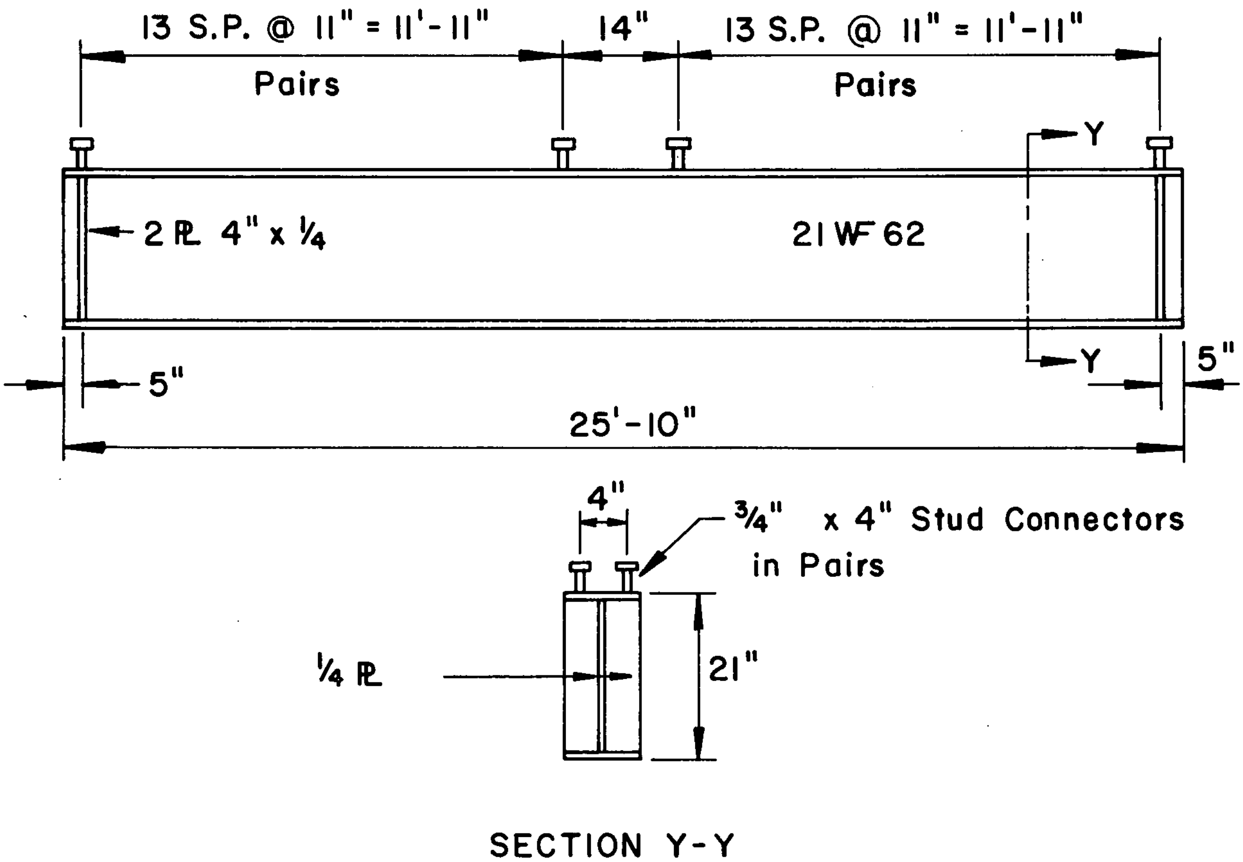

FIG. 3 - DETAILS OF STEEL BEAMS

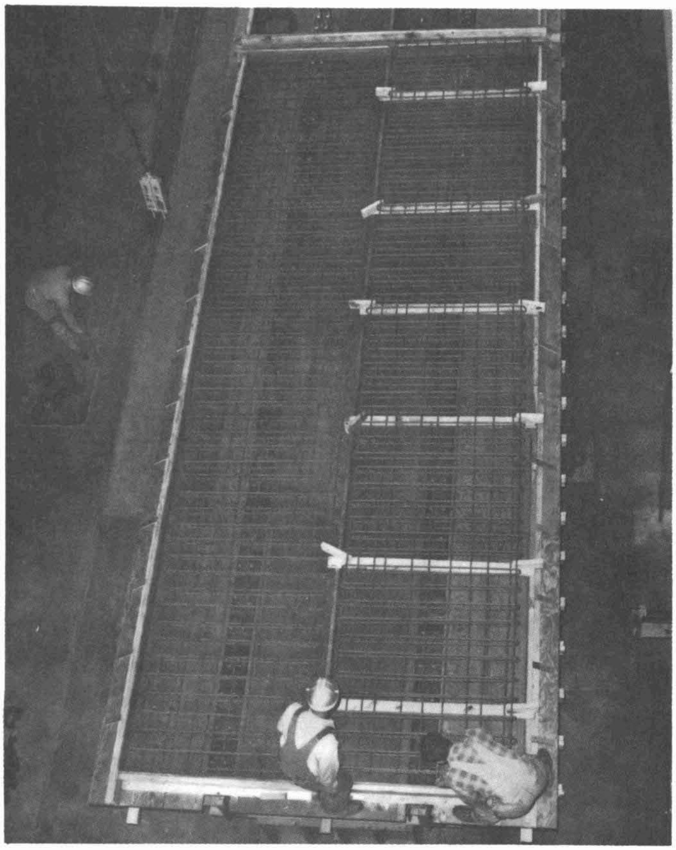

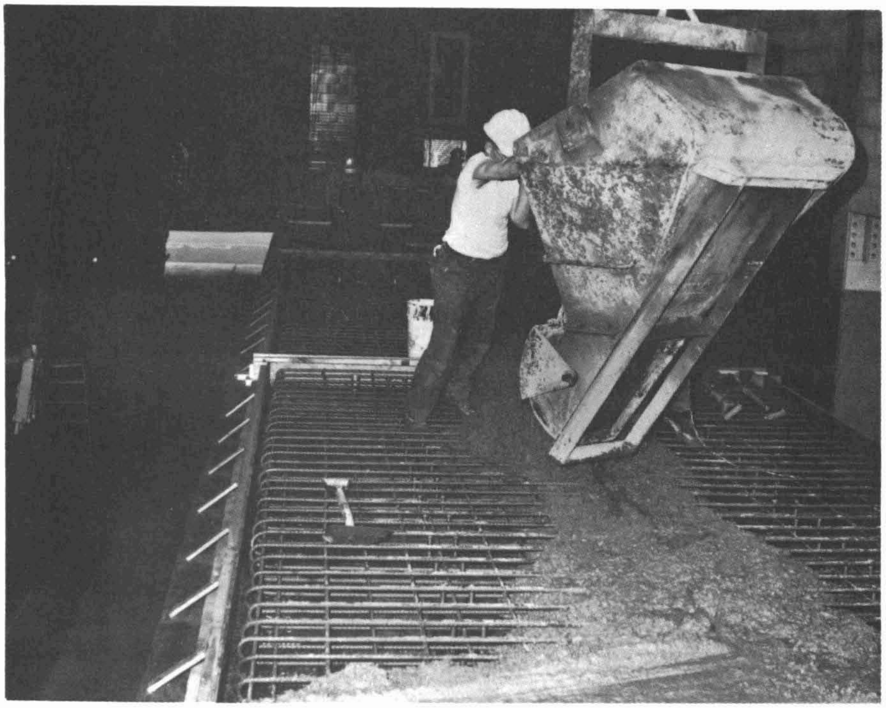

FIG. 4 - CONSTRUCTION OF COMPOSITE BEAMS

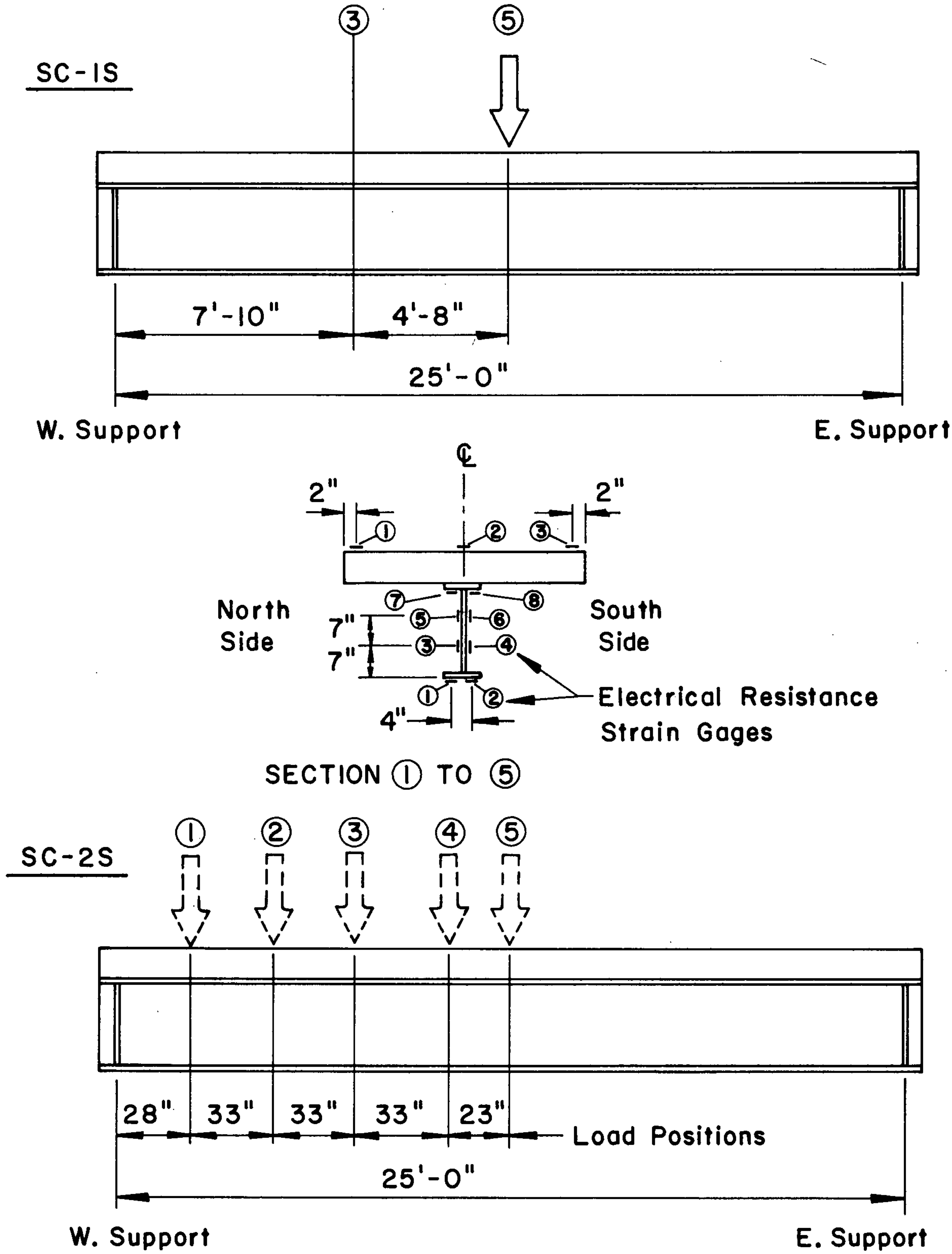

FIG. 5 - STRAIN GAGE LOCATIONS

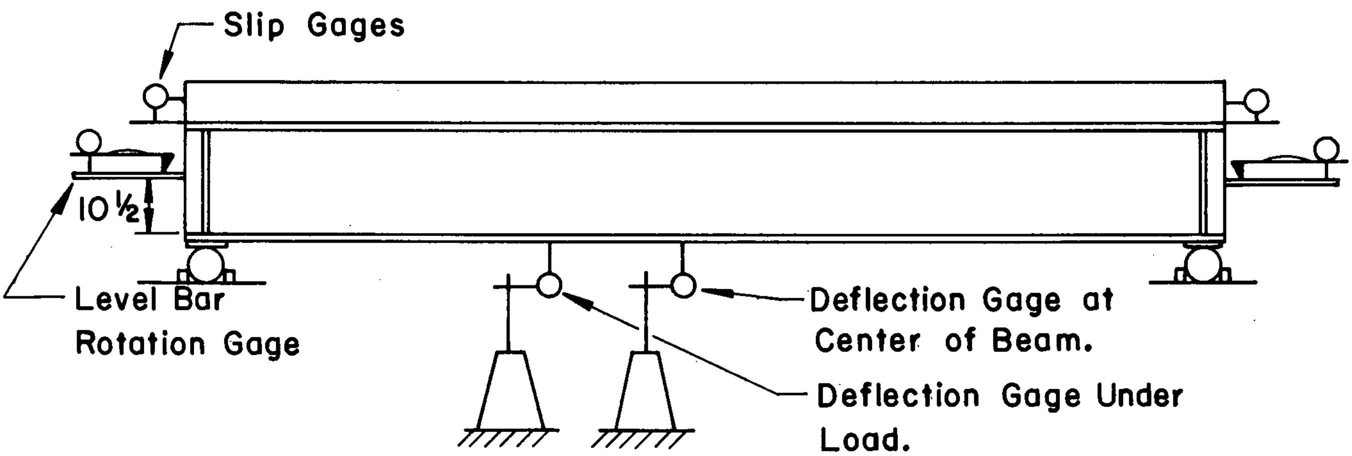

FIG. 6 - LOCATIONS OF DEFLECTION, ROTATION AND SLIP GAGES

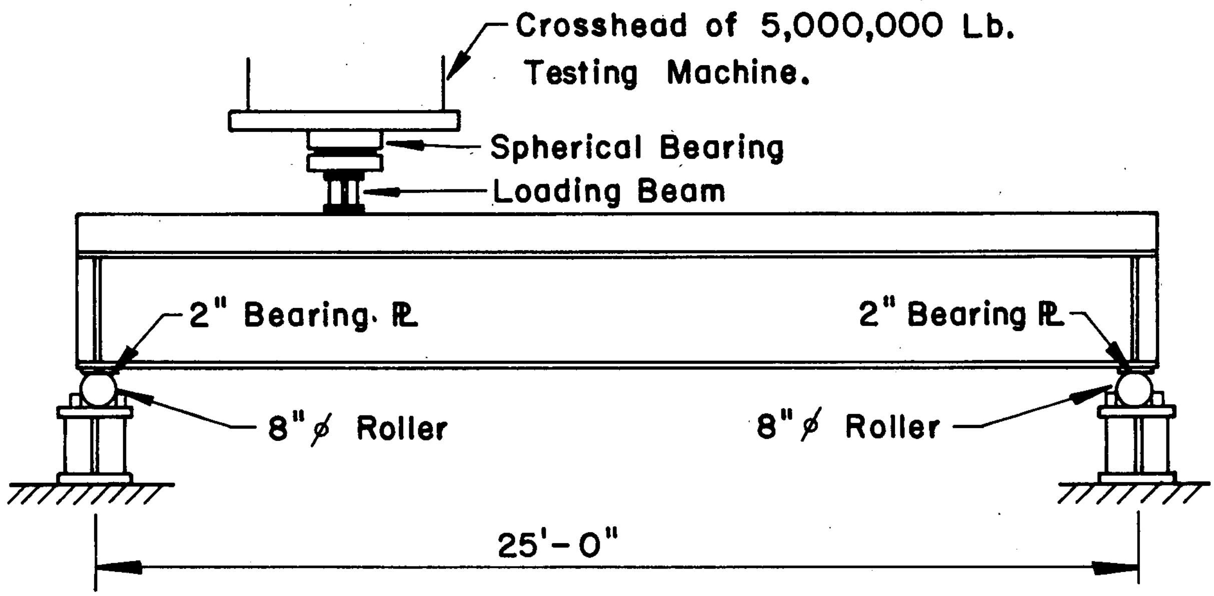

FIG. 7 - TEST SET-UP

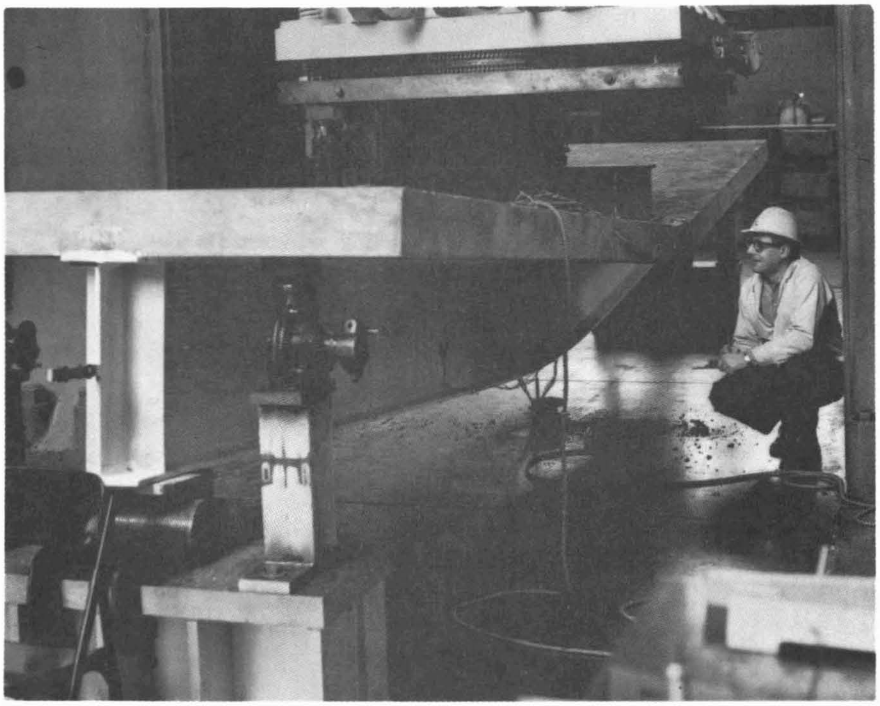

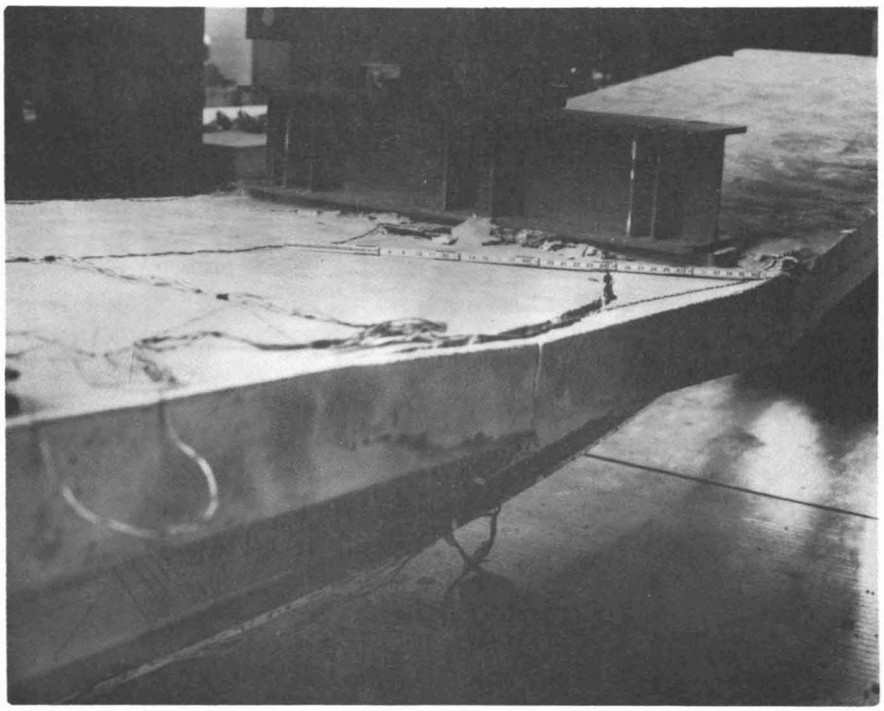

FIG. 8 - TEST OF BEAM SC-1S

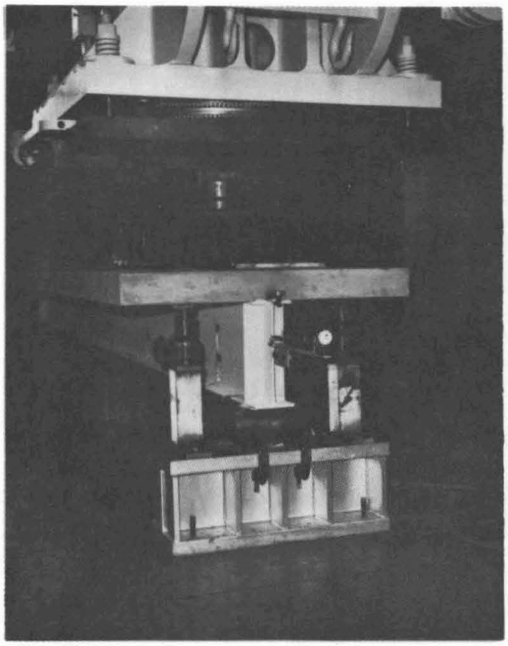

POSITION 1

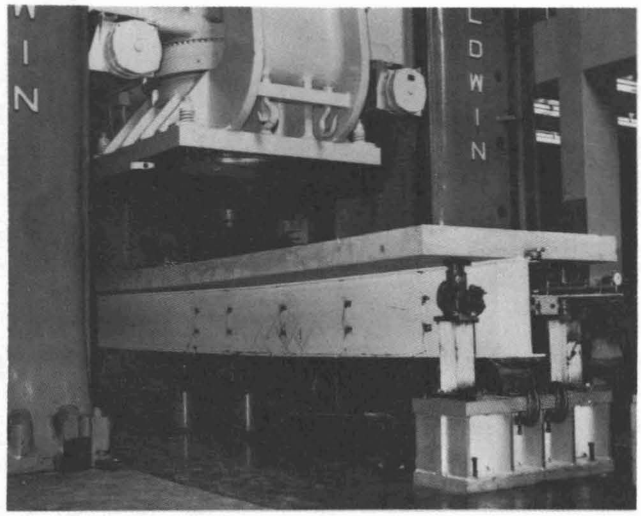

POSITION 4

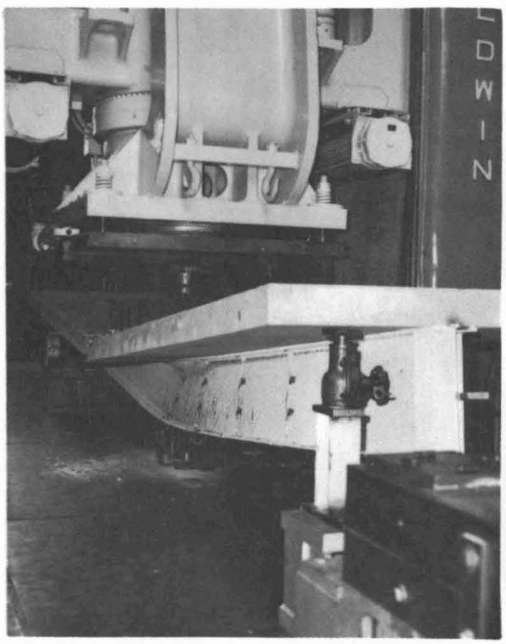

POSITION 5

POSITION 5

FIG. 9 -. TEST OF BEAM SC-2S

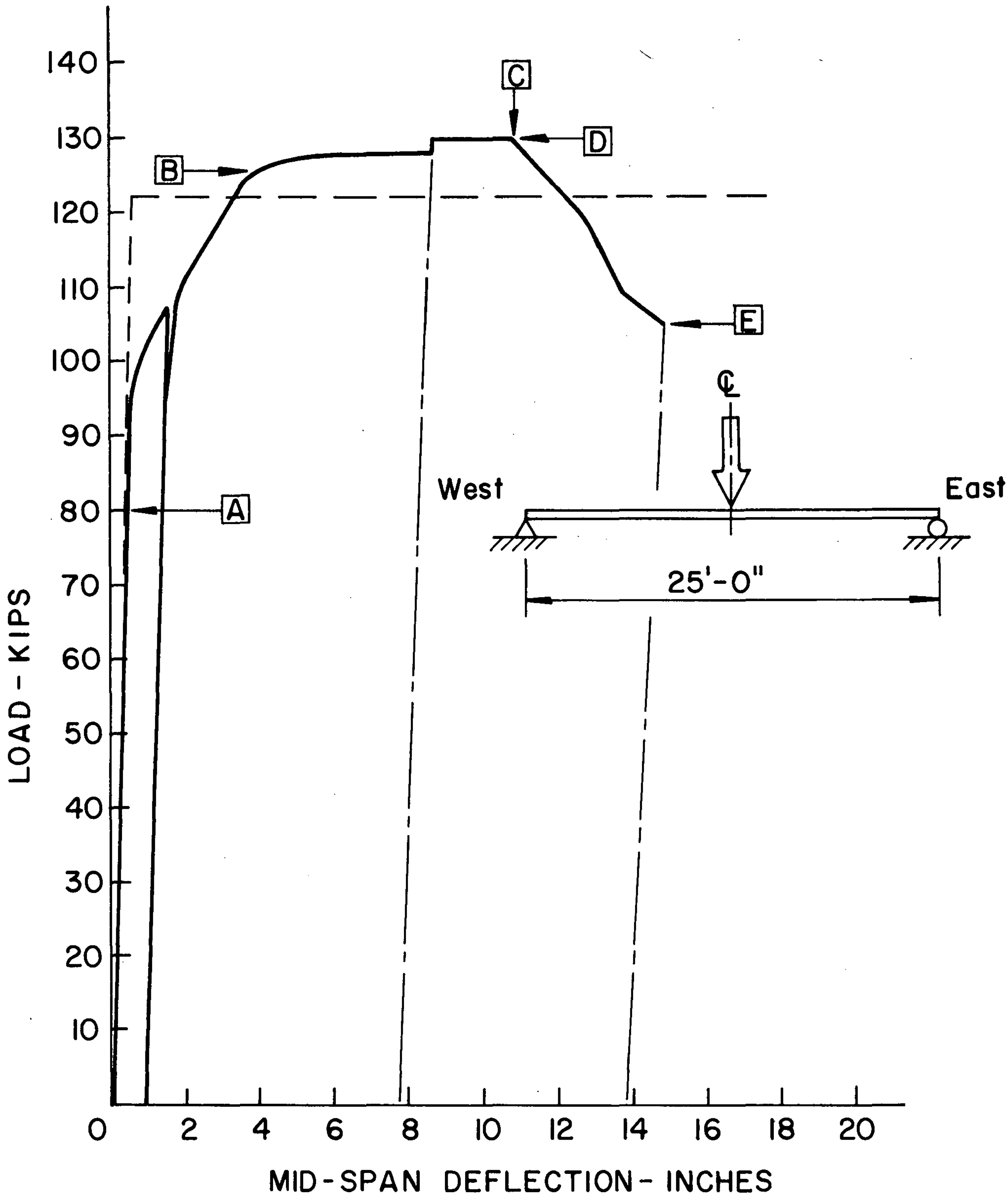

FIG. 10 - SC-1S: LOAD - DEFLECTION CURVES

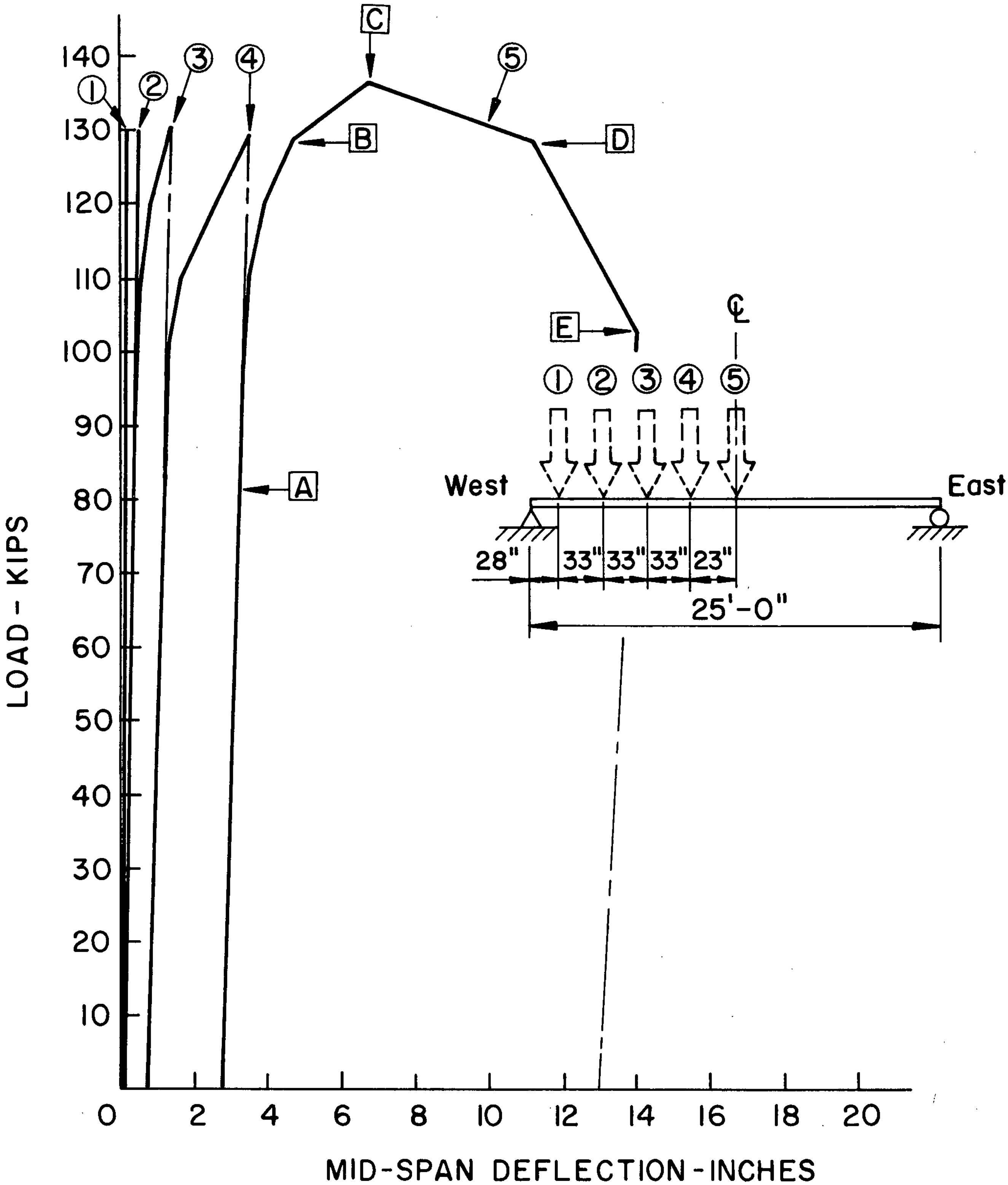

FIG. 11 - SC-2S: LOAD - DEFLECTION CURVES

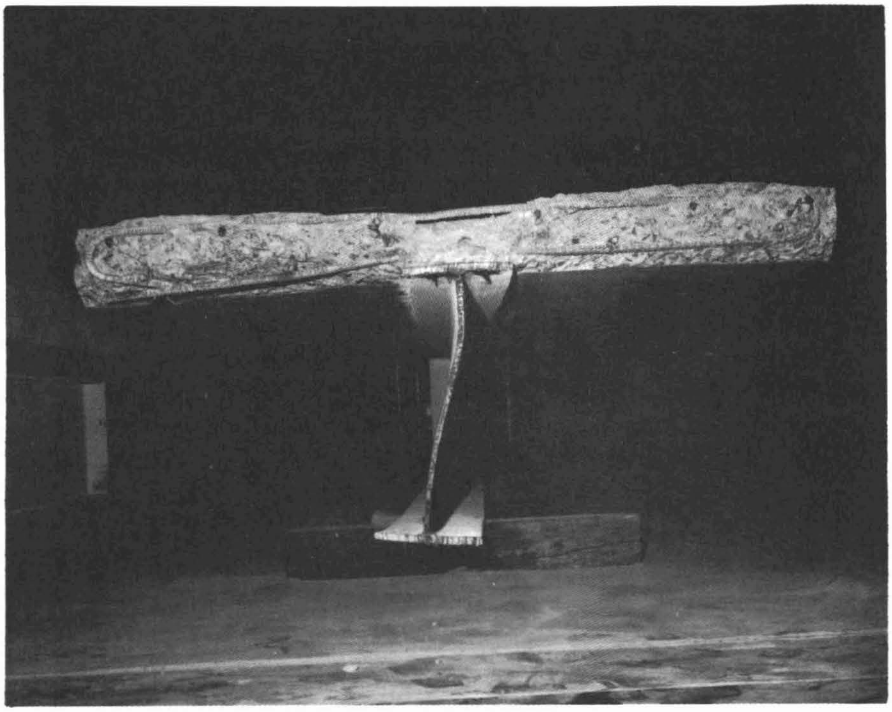

FIG. 12 - CROSS-SECTION OF BEAM SC-2S AT MID-SPAN AFTER TEST

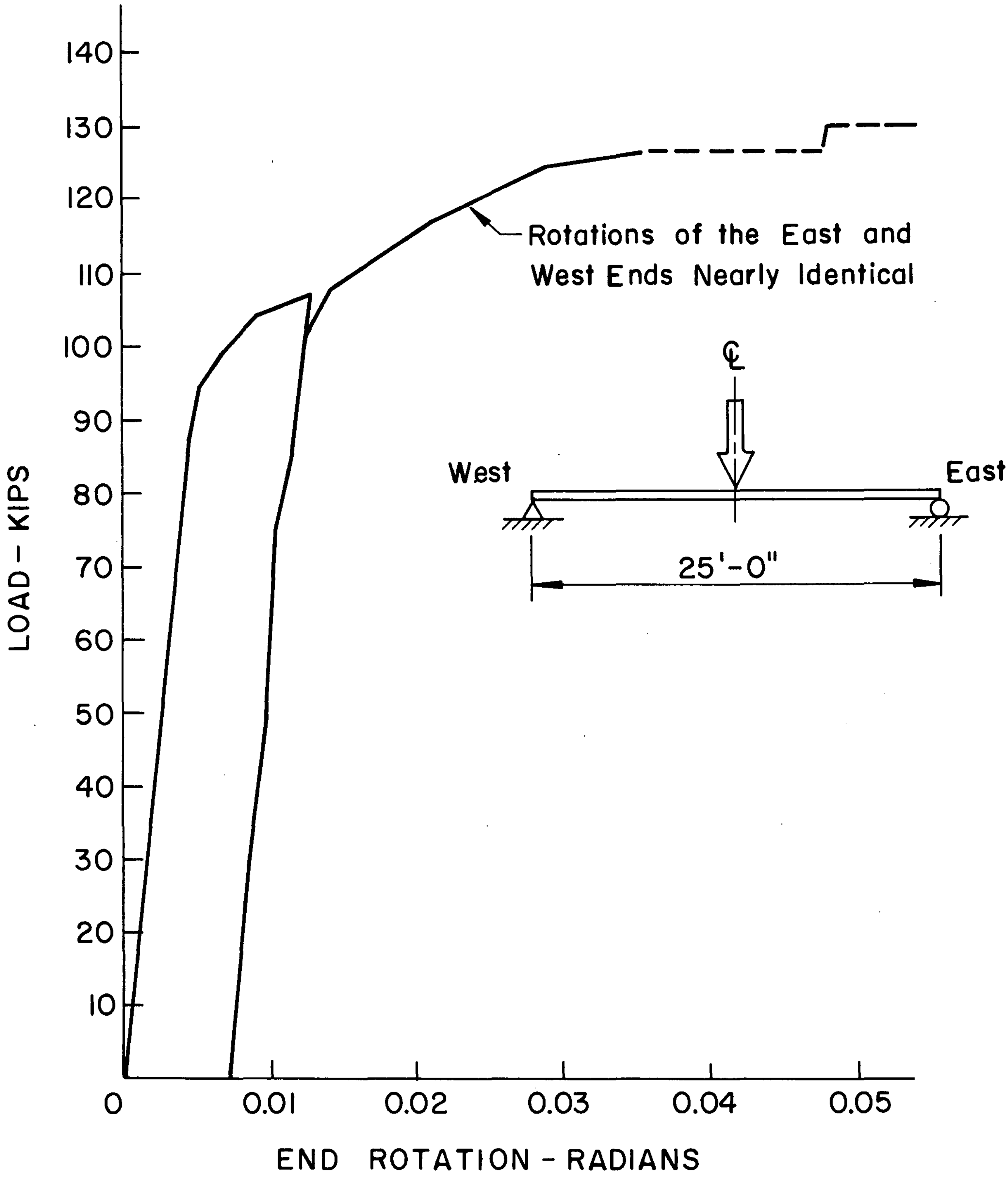

FIG. 13 - SC-1S: LOAD - ROTATION CURVES

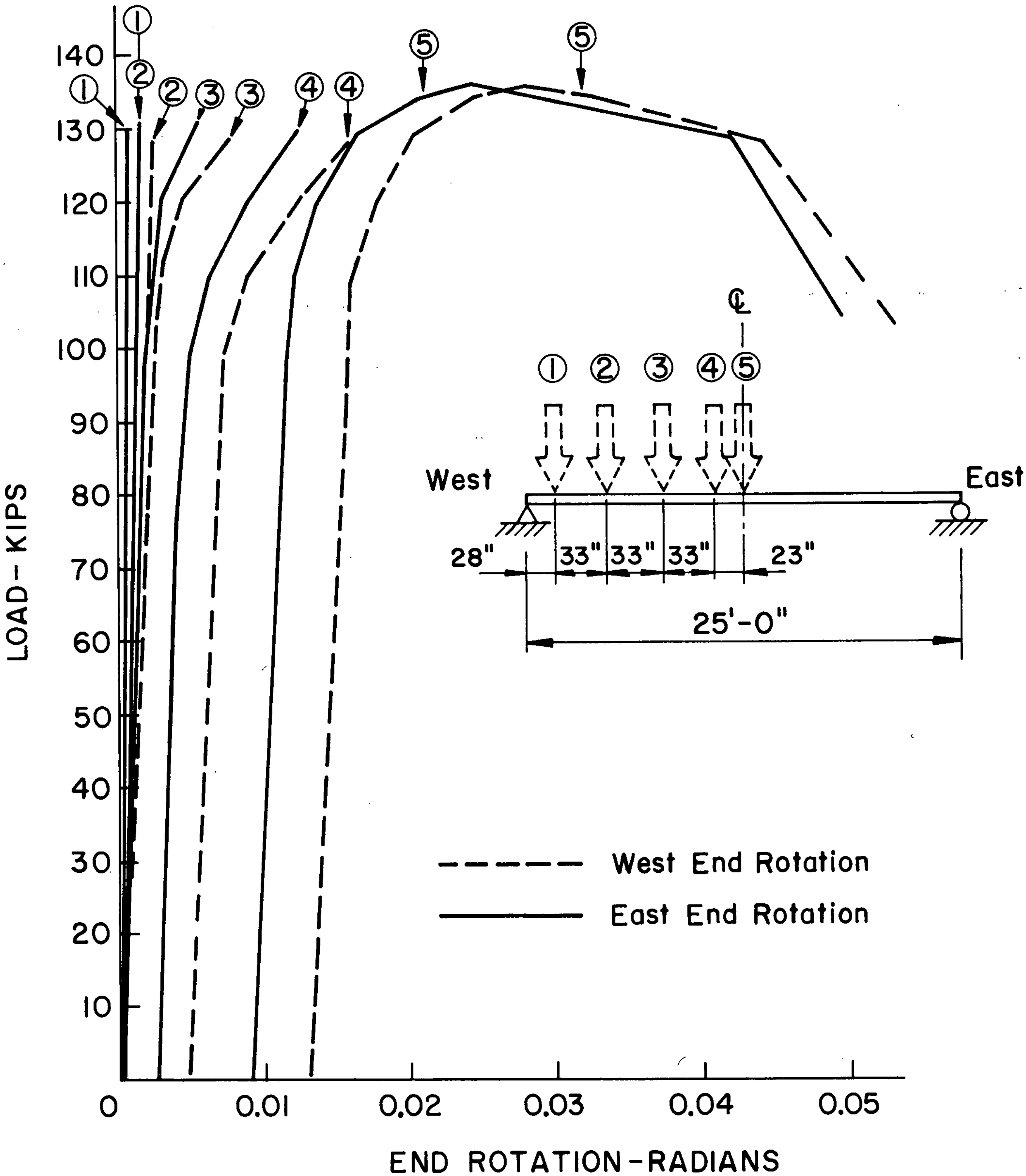

FIG. 14 - SC-2S: LOAD - ROTATION CURVES

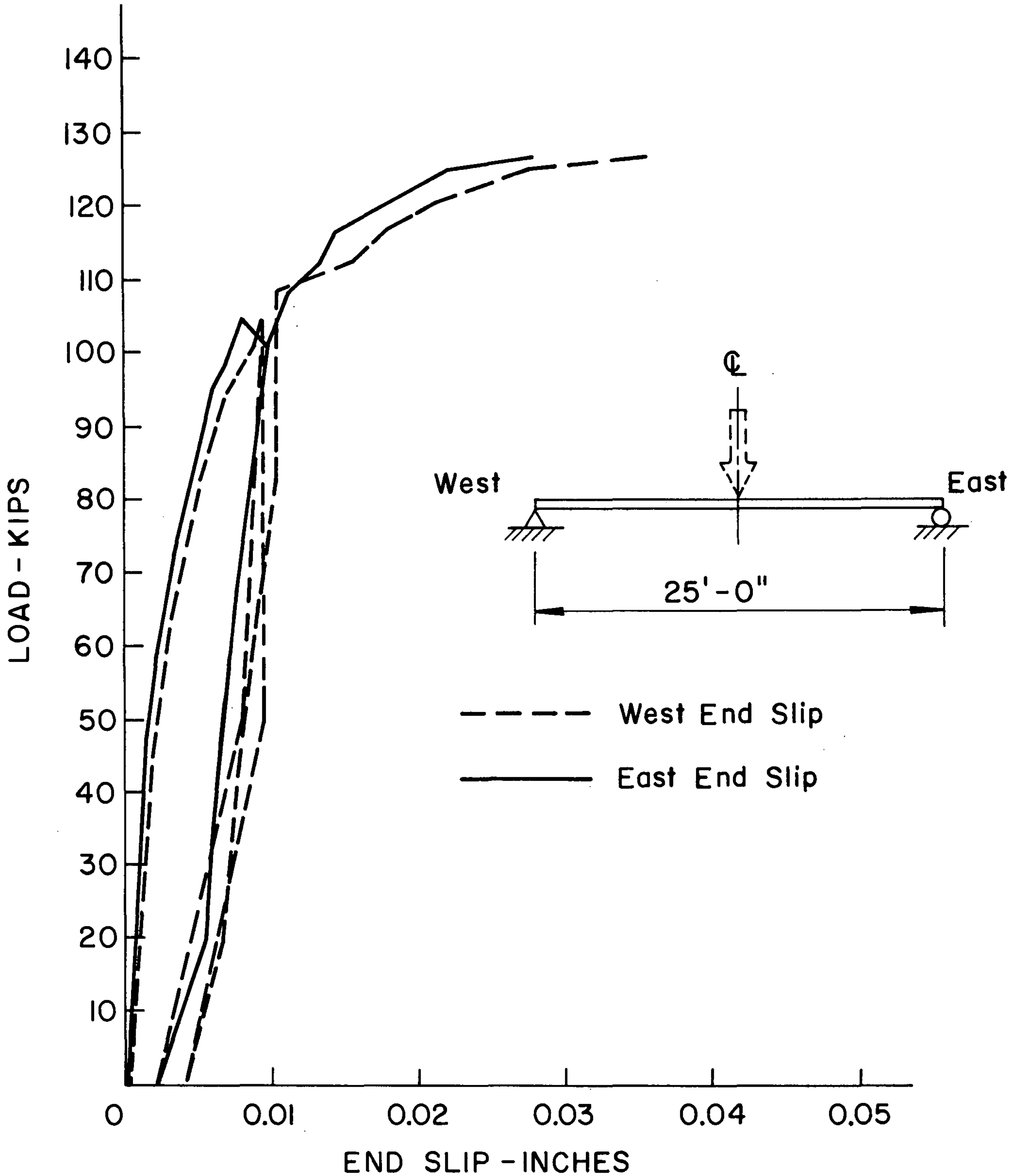

FIG. 15 - SC-1S: LOAD - SLIP CURVES

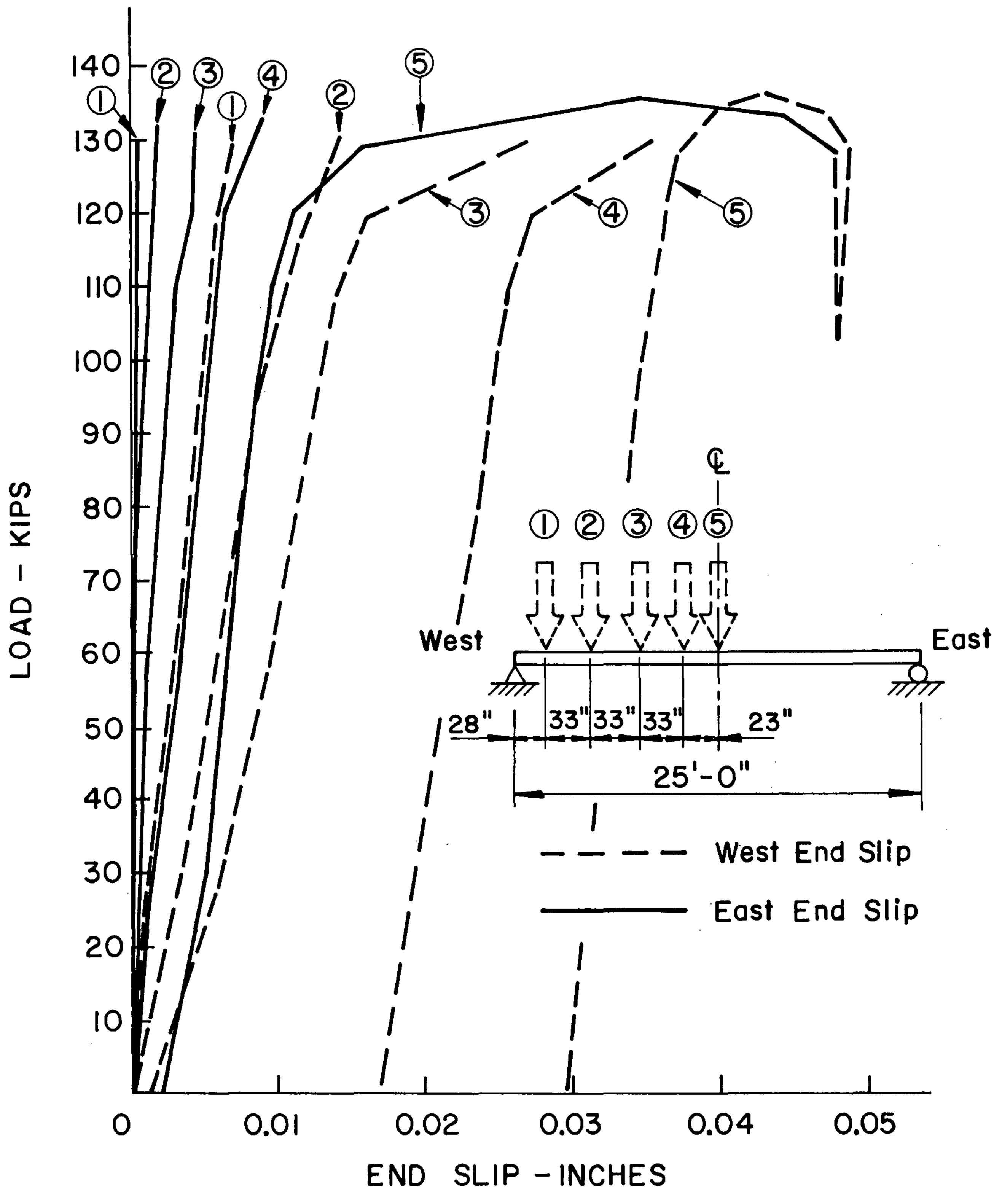

FIG. 16 - SC-2S: LOAD - SLIP CURVES

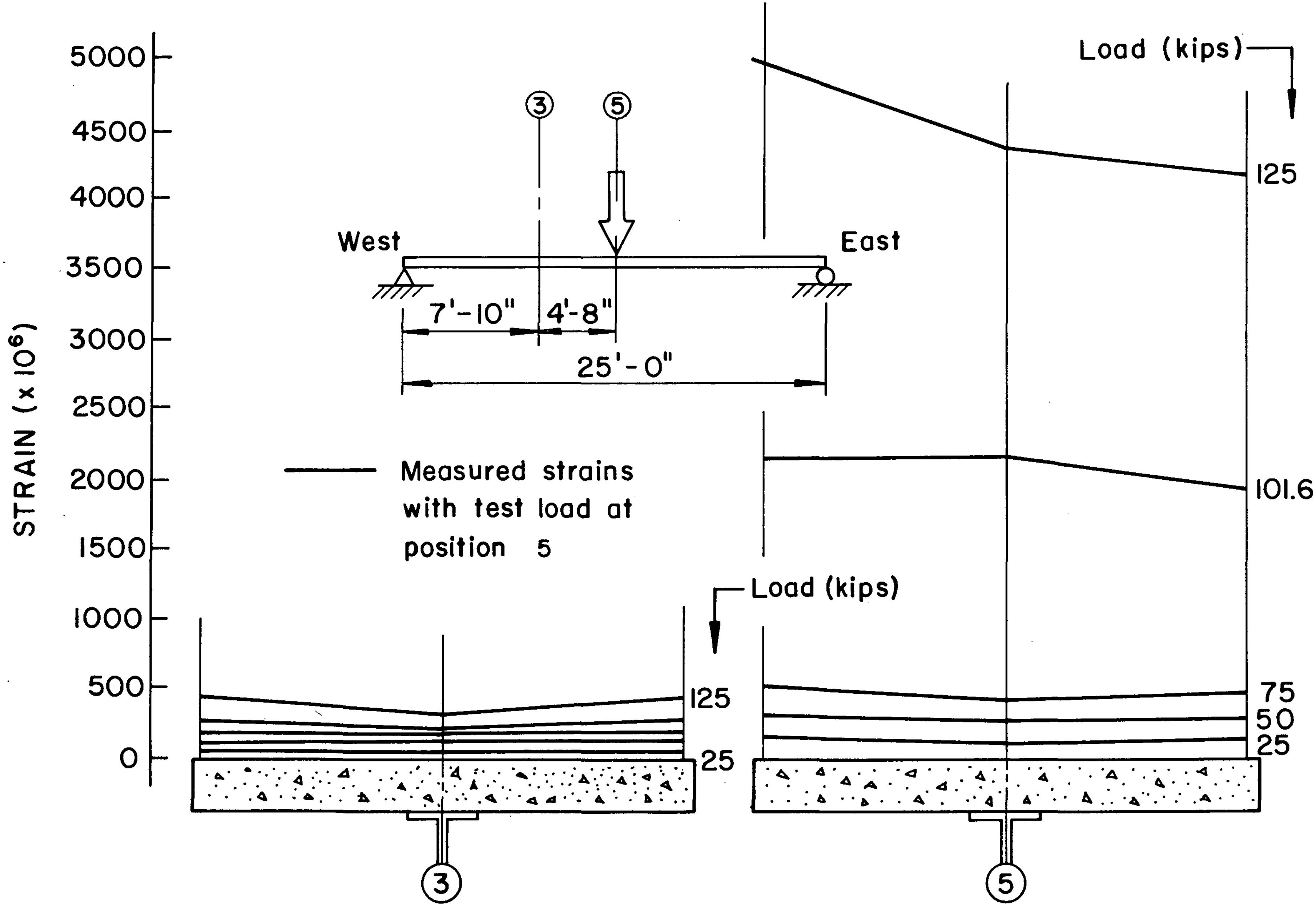

FIG. 17 - SC-1S: STRAIN DISTRIBUTION ACROSS SLAB

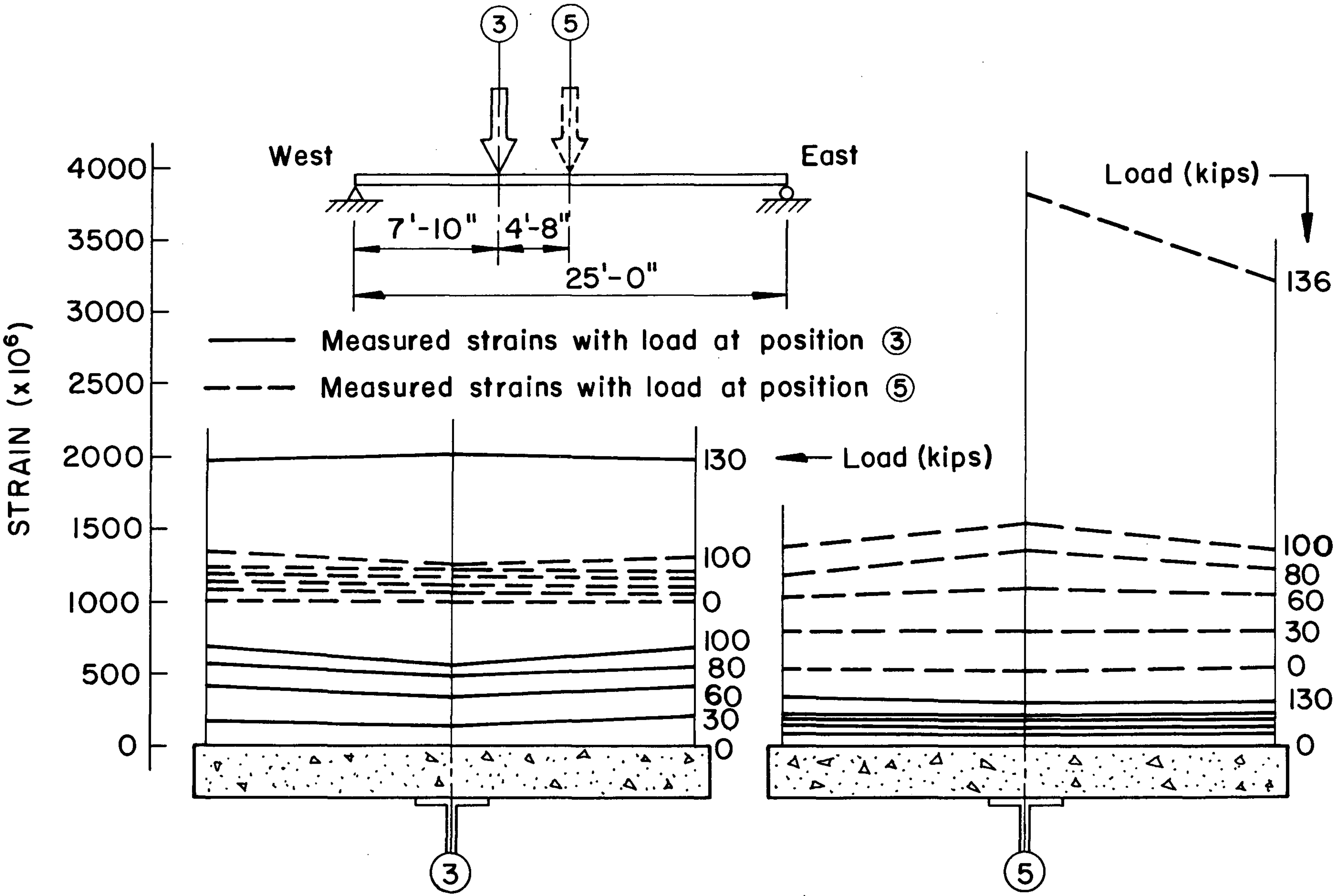

FIG. 18 - SC-2S: STRAIN DISTRIBUTION ACROSS SLAB

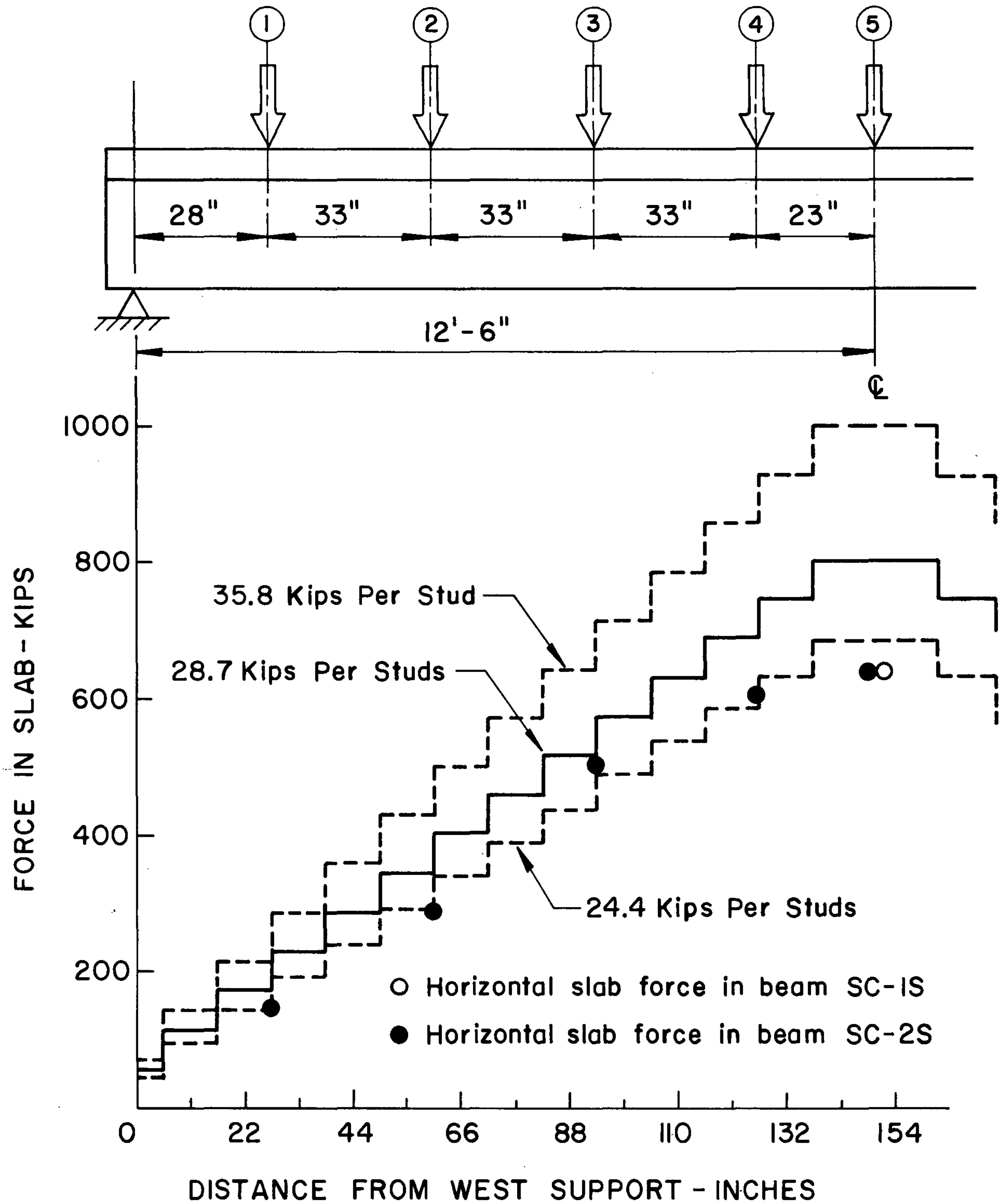

FIG. 19 - CUMULATIVE RESISTANCE OF STUD CONNECTORS FOR BEAMS SC-1S AND SC-2S

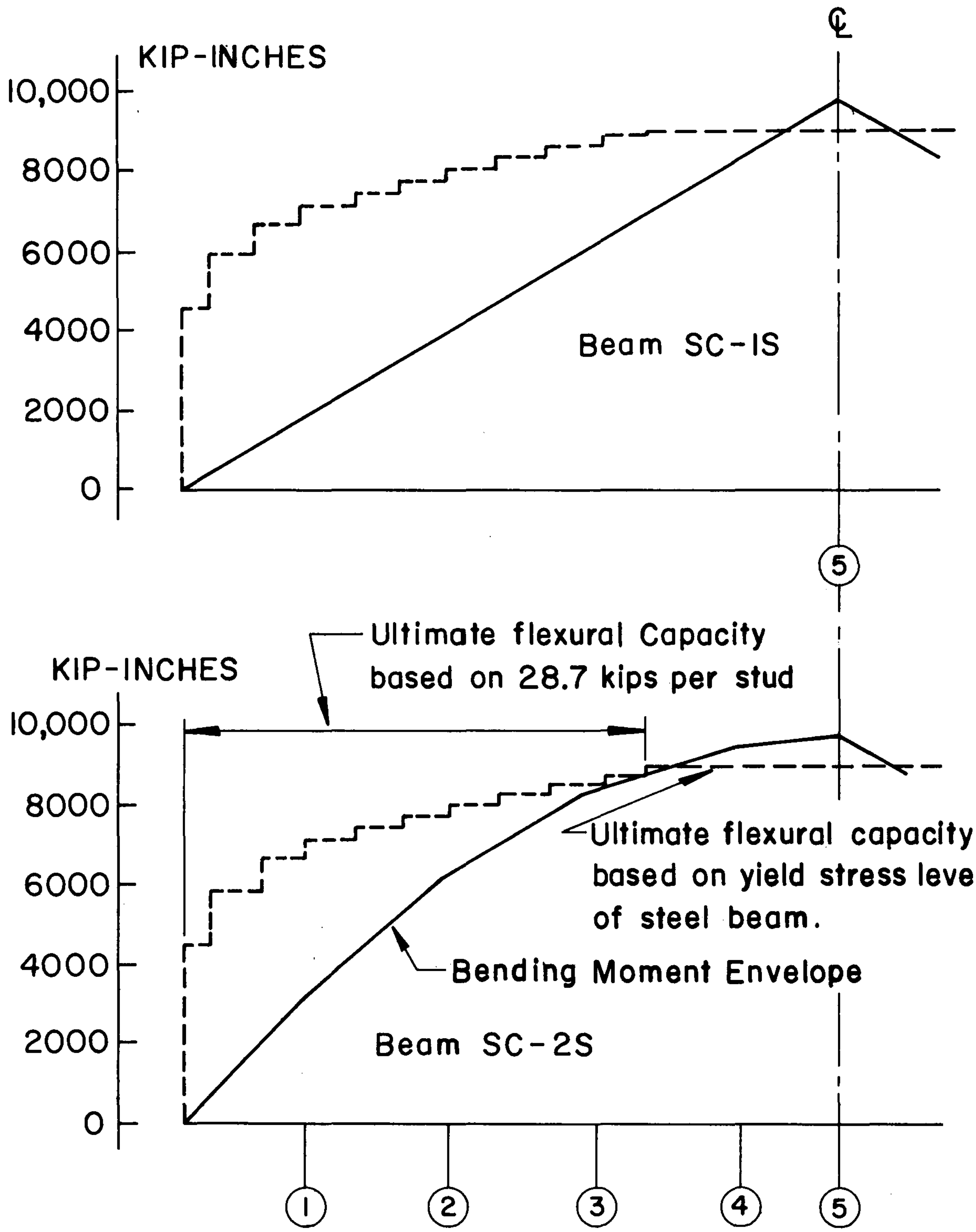

FIG. 20 - COMPARISON OF APPLIED MOMENTS WITH ULTIMATE FLEXURAL CAPACITY

7.0 REFERENCES

1. Slutter, R. G., and Fisher, J. W.
   FATIGUE STRENGTH OF SHEAR CONNECTORS, Highway Research Record No. 147, Highway Research Board, 1966, pp. 65-88

2. Slutter, R. G., and Driscoll, G. C. Jr.
   FLEXURAL STRENGTH OF STEEL-CONCRETE COMPOSITE BEAMS, Journal of the Structural Division, ASCE, Vol. 91, No. ST2, April 1965

3. Daniels, J. H., and Fisher, J. W.
   FATIGUE BEHAVIOR OF CONTINUOUS COMPOSITE BEAMS, Fritz Engineering Laboratory Report No. 324.1, Lehigh University, December 1966

4. Daniels, J. H., and Fisher, J. W.
   STATIC BEHAVIOR OF CONTINUOUS COMPOSITE BEAMS, Fritz Engineering Laboratory Report No. 324.2, Lehigh University, March 1967

5. Appendix C - Welding and Inspection of Stud Shear Connectors.
   RECOMMENDATIONS FOR THE DESIGN AND CONSTRUCTION OF COMPOSITE BEAMS AND GIRDERS FOR BUILDINGS. Report of the Joint ASCE - ACI Committee on Composite Construction, 1966

6. Johnson, R. P., Van Dalen, K., and Kemp, A. R.
   ULTIMATE STRENGTH OF CONTINUOUS COMPOSITE BEAMS, Progress Report, British Constructional Steelwork Association Conference, September 1966.